Electrochemically Controlled Assembling/Disassembling Processes with a Bis-imine Bis-quinoline Ligand and the Cu^{II}/Cu^{I} Couple

Valeria Amendola,[a] Luigi Fabbrizzi,*[a] Laura Linati,[b] Carlo Mangano,[a] Piersandro Pallavicini,[a] Valentina Pedrazzini,[a] and Michele Zema[b]

Abstract: The bis-iminoquinoline quadridentate ligand **L** is capable of forming air- and moisture-stable complexes both with Cu^{II} and Cu^{I}; thus the $\mathbf{L}/Cu^{II/I}$ set is a bistable system. Owing to its quite rigid preorganized structure, **L** forms the 1:1 complex $[Cu^{II}\mathbf{L}]^{2+}$ when binding the d^9 cation Cu^{2+}, while with the d^{10} cation Cu^{+}, dimeric complexes of the $[Cu^{I}_2\mathbf{L}_2]^{2+}$ type are formed in which each copper cation is coordinated by two iminoquinoline fragments belonging to two different ligands. Crystal and molecular structure determinations showed that, in $[Cu^{II}\mathbf{L}](CF_3SO_3)_2$, **L** binds to the metal center in a square-planar fashion, while in $[Cu^{I}_2\mathbf{L}_2](CF_3SO_3)_2$ the Cu^{+} cations are coordinated with a tetrahedral geometry, with the two ligands **L** intertwined in a double helix. On the other hand, in the case of $[Cu^{I}_2\mathbf{L}_2](ClO_4)_2$ both a helical species and a dimeric nonhelical one were found to coexist *in the same crystal cell*. However, spectrophotometric and ^1H NMR studies demonstrated that, in acetonitrile solution, only two helical forms exist, one of which is more prevalent (87%, at 20 °C). The interconversion equilibrium between the two helical forms has been studied in acetonitrile by temperature variable ^1H NMR and the pertinent $\Delta H^{\ominus}$ and $\Delta S^{\ominus}$ values have been determined; these account for the small difference in energy between the two species. Finally, cyclic voltammetry and spectroelectrochemical experiments demonstrated that in acetonitrile solution it is possible to rapidly transform $[Cu^{II}\mathbf{L}]^{2+}$ into the helical $[Cu^{I}_2\mathbf{L}_2]^{2+}$ dimer (or vice versa) by changing the potential applied to the working electrode, that is, it is possible to electrochemically control the self-assembly/disassembly process through the Cu^{II}/Cu^{I} redox couple. Moreover, it has been shown that self-assembly (reduction)/disassembly (oxidation) cycles can be repeated at will, without any degradation of the system.

Keywords: copper · electrochemistry · helicates · molecular devices · self-assembly

Introduction

Although self-assembled structures (boxes,[1] cylinders,[2] racks[3] and, among many others, helices[4] in particular) have been thoroughly investigated by the supramolecular chemists, much less has been done about the control of the self-assembly process, that is, the process taking place in a fast and reversible way (in a solution containing a mixture of the fragments to be assembled), following an external input. On the other hand, the use of molecular switches[5] (electrochemical, in particular) has been introduced in the last decade; this has lead to a lot of interesting multi-component molecules including *molecular machines*,[6] that is, systems in which one component can be switched between two topologically different states, either by making a fragment move with respect to the whole molecule or by making the whole molecule rearrange between two significantly different conformations. By merging the results obtained in these two fields one should be able to find ways to control the self-assembly of a molecule by means of a switch. However, few works moving along this concept have been published. In 1984, Lehn, Sauvage and others described a *p*-quaterpyridine/$Cu^{II/I}$ system in which the self-assembly/disassembly of a double helix could be electrochemically controlled:[7] starting from a monomeric complex of Cu^{II}, the dimeric Cu^{I} double-helicate self-assembled by electrochemical reduction by a fast process. The disassembled, monomeric Cu^{II} complex was regenerated by electrochemical oxidation, although through a much slower process. In 1993, Abruña, Potts and others described a similar system,[8a] consisting of a quaterpyridine ligand (bearing -SR substituents) and a $Cu^{II/I}$ cation; the authors were again able to electrochemically switch from a Cu^{II} monomeric complex to a dimeric, double-helical Cu^{I} complex by a process that was fast in both directions. Moreover, the same authors described other, more complicated helical systems[8b] made from quin-

[a] Prof. L. Fabbrizzi, Dr. V. Amendola, Dr. C. Mangano
Dr. P. Pallavicini, Dr. V. Pedrazzini
Dipartimento di Chimica Generale, Università di Pavia
via Taramelli 12, I-27100 Pavia (Italy)
Fax: (+390) 382-528544
E-mail: fabbrizz@unipv.it

[b] Dr. L. Linati, Dr. M. Zema
Centro Grandi Strumenti, Università di Pavia, via Bassi 21
27100 Pavia (Italy)

  0947-6539/99/0512-3679 $ 17.50+.50/0

que- or sexipyridine ligands plus a series of transition metal cations. Changing the oxidation state of the latter, the overall molecular conformation was made to change, although an intertwined architecture persisted in all cases.

In this work, we report a new example, well within this field, based on the $Cu^{II/I}$ couple and on a ligand, **L**, that features quinoline and imine fragments, that is, sp^2 nitrogen donors that belong to an extended π-system, which displays comparable affinity towards both Cu^{II} and Cu^{I}. Moreover, the quite rigid tetradentate ditopic molecule **L**, consisting of two imino-quinoline (ImQ) halves separated by a cyclohexane spacer (substituted in 1,2 positions, with a *trans* conformation), was chosen in view of its straightforward preparation and its ability to chelate a single cation (for example Cu^{II}) in a square-planar geometry, but not to "close" on a metal cation which requires a tetrahedral coordination geometry (for example Cu^{I}). In the latter case, a dimeric structure is obtained, in which the chosen cation attains its more favourable coordination geometry (tetrahedral), by binding two ImQ halves belonging to two different molecules, possibly by assembling them in a helical arrangement. Crystal structures of the Cu^{I} and Cu^{II} complexes with **L** are reported; they demonstrate the existence of the expected monomeric $[Cu^{II}\mathbf{L}]^{2+}$ and dimeric helical $[Cu^{I}_2\mathbf{L}_2]^{2+}$ species. Moreover, it is also possible to achieve fast assembly of the dimeric $[Cu^{I}_2\mathbf{L}_2]^{2+}$ species from $[Cu^{II}\mathbf{L}]^{2+}$ by electrochemical oxidation and, vice versa, to achieve fast disassembly of the dimeric $[Cu^{I}_2\mathbf{L}_2]^{2+}$ complex to give back the Cu^{II} monomer on electrochemical reduction; this cycle can be repeated at will without any degradation. Finally, single-crystal X-ray diffraction studies have focussed on the $[Cu^{I}_2\mathbf{L}_2]^{2+}$ dimer and reveal that, in the solid state, it can exist in different conformations (depending on the counter anion). In particular, a nonhelical and a helical $[Cu^{I}_2\mathbf{L}_2]^{2+}$ molecular cation have been found to exist in the same crystal, even if in CH_3CN and CH_3OH solution only one helical form prevails, as shown by ^1H NMR spectroscopic studies.

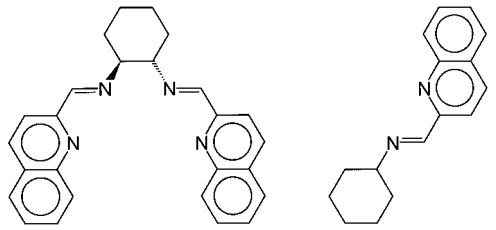

L L'

Abstract in Italian: *Il legante quadridentato **L** forma sia con Cu^{II} che con Cu^{I} complessi stabili all'aria e all'umidità. Per via della sua struttura rigida, **L** dà con il catione d^9 Cu^{II} un complesso a stechiometria 1:1, $[Cu^{II}\mathbf{L}]^{2+}$, mentre con il catione Cu^{I}, d^{10}, forma complessi dimeri di formula $[Cu^{II}_2\mathbf{L}_2]^{2+}$, nei quali ciascun centro metallico è coordinato da due frammenti imminochinolinici appartenenti a due differenti molecole di legante. Studi cristallografici sul composto $[Cu^{II}\mathbf{L}](CF_3SO_3)_2$ hanno mostrato che **L** è coordinato al metallo secondo una geometria quadrata, mentre nel composto $[Cu^{I}_2\mathbf{L}_2](CF_3SO_3)_2$ i cationi Cu^{+} sono coordinati secondo una stereochimica tetraedrica, con i due leganti avvolti a dare una doppia elica. D'altra parte, nel caso di $[Cu^{I}_2\mathbf{L}_2](ClO_4)_2$, si è osservato che coesistono nella stessa cella cristallografica sia una specie a elica che una specie dimera non elicoidale. Tuttavia, indagini spettrofotometriche e di spettroscopia ^1H NMR hanno dimostrato che in soluzione di acetonitrile sono presenti solamente due distinte specie a elica, delle quali una è nettamente prevalente (87 %, a 20 °C). L'equilibrio di interconversione tra le due forme a elica è stato studiato attraverso l'esperimento ^1H NMR a temperatura variabile, così da determinare i corrispondenti valori di $\Delta H^{\ominus}$ e $\Delta S^{\ominus}$: tali valori indicano che le due specie sono separate da una piccola differenza di energia. Infine, studi di voltammetria ciclica ed esperimenti spettroelettrochimici in acetonitrile hanno dimostrato che è possibile trasformare rapidamente $[Cu^{II}\mathbf{L}]^{2+}$ nel dimero a elica $[Cu^{I}_2\mathbf{L}_2]^{2+}$ (o viceversa), variando opportunamente il potenziale dell'elettrodo di lavoro; in altre parole, è possibile controllare per via elettrochimica il processo di avvolgimento/svolgimento dell'elica attraverso la coppia redox Cu^{II}/Cu^{I}. E' stato mostrato inoltre che cicli di avvolgimento (riduzione)/svolgimento (ossidazione) possono essere ripetuti a piacere, senza degradazione alcuna del sistema.*

Results and Discussion

Synthesis and product stability: Ligand **L** and its Cu^{I} and Cu^{II} complexes represent a very easily attainable and genuine bistable system. In contrast to the quaterpyridine ligands used so far for the interconversion between monomeric Cu^{II}/dimeric (helical) Cu^{I} complexes, which can be prepared only through multistep syntheses,[9, 10] **L** can be obtained in an 80 % yield thanks to a one step Schiff condensation, starting from commercially available products. Besides its easy availability, **L** has been chosen on the basis of two considerations.

1) A ligand was needed that features donor atoms suitable for coordination to both Cu^{I} and Cu^{II}, for example, sp^2 nitrogens belonging to an extended π-system.
2) The ligand had to display such a rigid, preoriented structure so that it could "close" on a single metal cation so that the metal has square planar rather than tetrahedral coordination. In the case of **L**, this is guaranteed by the rigid nature of the cyclohexyl fragment and of the two ImQ binding halves of the molecule.

Moreover, the 1,2-substituted cyclohexane fragment was chosen as its *trans* isomer, with the idea that when a cation needing a tetrahedral coordination was added to **L**, two **L** ligands would have to coordinate to two metal centres (each tetrahedral metal centre coordinated by two ImQ halves belonging to two different molecules). This is favoured by the torsion angle (N–C–C–N) between the imine nitrogens in each **L**,[11] which should also make it easier for the two ligands to intertwine one with another and give a helical complex. Finally, a quinoline fragment (instead of, for example, pyridine) was chosen to give to the Cu^{I} and Cu^{II} complexes an increased thickness and lipophilicity, in order to minimize the possibility of reaction at the metal centres or at the imine group with O_2 and H_2O.

0947-6539/99/0512-3680 $ 17.50+.50/0 *Chem. Eur. J.* **1999**, *5*, No. 12

Both Cu^{I} and Cu^{II} complexes may be obtained in high yields as pure crystals by mixing **L** with stoichiometric quantities of metal salts in acetonitrile or methanol, with no particular regard towards O_2 or H_2O exclusion (for example, 95% ethanol can also be used as the solvent). Moreover, the isolated $[Cu^{II}\mathbf{L}](CF_3SO_3)_2$ and $[Cu^{I}_2\mathbf{L}_2](CF_3SO_3)_2$ complexes appear to be stable on exposure to air or moisture. The monomeric or dimeric nature of the Cu^{II} and Cu^{I} compounds in the solid state was demonstrated by single-crystal X-ray diffraction analysis and in solution by mass spectra experiments and spectrophotometric titrations in acetonitrile. Addition of substoichiometric quantities of $[Cu^{I}(CH_3CN)_4]ClO_4$ or $Cu(CF_3SO_3)_2$ to an acetonitrile solution of **L** resulted in the growth of bands centred at 536 nm ($\varepsilon = 3500\ mol^{-1}\,L\,cm^{-1}$; CT) in the case of Cu^{I} and 336 nm ($\varepsilon = 12000\ mol^{-1}\,L\,cm^{-1}$; CT) and 668 nm ($\varepsilon = 105\ mol^{-1}\,L\,cm^{-1}$; d–d transition) in the case of Cu^{II}. When a ligand/metal molar ratio of one was reached, a spectrum was obtained that was superimposable to that measured on authentic samples of solid $[Cu^{I}_2\mathbf{L}_2](CF_3SO_3)_2$ {or $[Cu^{I}_2\mathbf{L}_2](ClO_4)_2$} and $[Cu^{II}\mathbf{L}](CF_3SO_3)_2$ dissolved in the same solvent. Further addition of metal salts, up to a **L**/metal molar ratio of 1:3, did not modify the observed spectrum; this implies that the obtained complex cations do not rearrange to distribute their donor atoms and interact with the excess metal cations. The mass of the molecular cations present both in 1:1 **L**/metal cation solutions and on solution of authentic samples of solid $[Cu^{I}_2\mathbf{L}_2](CF_3SO_3)_2$ and $[Cu^{II}\mathbf{L}](CF_3SO_3)_2$ was checked with MS-ESI experiments; peaks were observed at 1059 and 604, which are the expected values for $\{[Cu^{I}_2\mathbf{L}_2]+CF_3SO_3\}^+$ and $\{[Cu^{II}\mathbf{L}]+CF_3SO_3\}^+$, respectively.

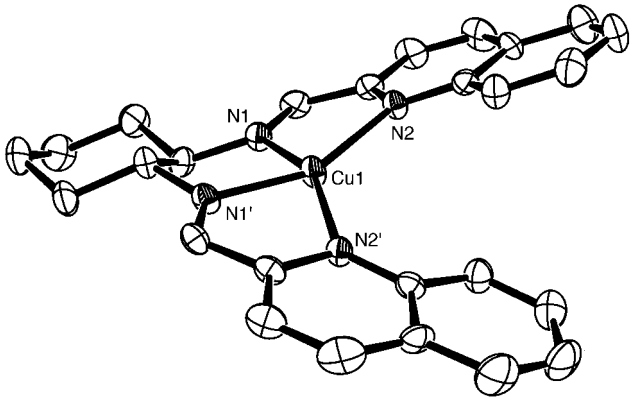

Figure 1. ORTEP view of $[Cu^{II}\mathbf{L}](CF_3SO_3)_2$ with 30% probability displacement ellipsoids. The triflate anions have been omitted for clarity. Selected bond lengths: Cu1–N1 1.956(5); Cu1–N2 2.091(5). Selected angles: N1–Cu1–N1^{i} 80.7(3)°; N1–Cu1–N2 80.1(2)°; N2–Cu1–N2^{i} 122.4(3)°. Symmetry codes: (i) $-x+1, y, -z+3/2$.

Structures in the solid state

$[Cu^{II}\mathbf{L}](CF_3SO_3)_2$: The crystal and molecular structure of the Cu^{II} complex was determined by X-ray diffraction methods. The Cu atom lies on a twofold rotation axis parallel to the *b* crystallographic direction and also passes through the midpoints of the C11-C11^{i} and C13-C13^{i} bonds in cyclohexane so that the two halves of the **L** ligand are related by this symmetry element (Figure 1).

As a consequence, half of the formula unit comprises the asymmetric unit. The Cu^{II} cation is coordinated by the four nitrogen atoms of a single **L** ligand, with two Cu–N (imine) bond lengths of 1.956(5) Å and two Cu–N (quinoline) bond lengths of 2.091(5) Å. Three N–Cu–N angles are $\approx 80°$ and one, which involves the two quinoline nitrogen atoms, is $\approx 120°$. Moreover, the coordination sphere of the copper cation also includes two oxygen atoms of the two triflate anions; these lie in the apical positions of a very elongated octahedron [Cu–O 2.431(4) Å] and form an angle O1-Cu-O1^{i} of 159.8(2)°. While one has to describe the overall geometry of Cu^{II} as distorted tetragonal, the positioning of the four nitrogen atoms of ligand **L** around Cu^{II} can be seen as square planar, with a small but significant distortion towards tetrahedral. The Cu atom lies only 0.03 Å above the N_4 mean-plane, but the four nitrogen atoms are displaced with respect to the plane with distances ranging from 0.13 to 0.36 Å. Besides the van der Waals forces, the crystal is maintained by weak C–H···O interactions [C1···O2^{ii} 3.155(9) Å; H1···O2^{ii} 2.258(9) Å; C1–H1···O2^{ii} 161.8(7)°; C8···O3^{iii} 3.22(1) Å; H8···O3^{iii} 2.42(1); C8–H8···O3^{iii} 143.9(9)°; symmetry codes: (ii) $-x+1, -y, -z+2$; (iii) $-x+3/2, y+1/2, -z+2$].

$[Cu^{I}_2\mathbf{L}_2](CF_3SO_3)_2$: X-ray diffraction studies allowed us to determine the crystal and molecular structure of this compound, which, in the solid state, consists of separate $[Cu_2\mathbf{L}_2]^{2+}$ molecular cations and $CF_3SO_3^-$ anions (Figure 2); these

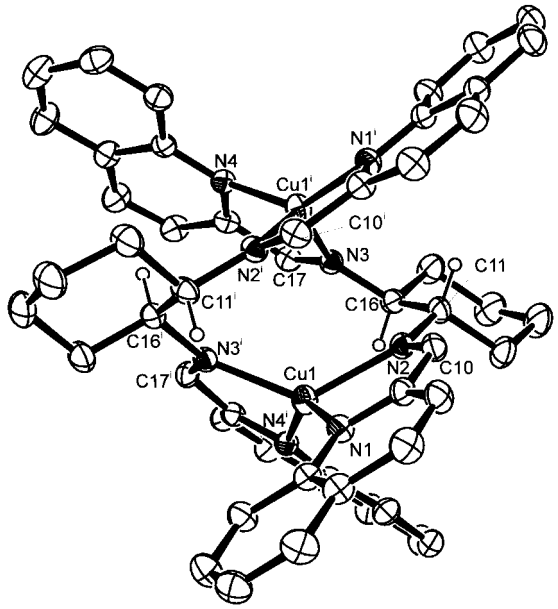

Figure 2. ORTEP view of $[Cu^{I}_2\mathbf{L}_2](CF_3SO_3)_2$ with 30% probability displacement ellipsoids. The triflate anions and the water molecule have been omitted for clarity. The asymmetric unit, both the Cu^{I} ions and the N atoms of the equivalent **L** ligand are labelled. Selected bond lengths: Cu1–N1 2.017(3) Å; Cu1–N2 2.096(3) Å; Cu1–N3^{i} 2.056(3) Å; Cu1–N4^{i} 2.041(3) Å. Selected angles: N1–Cu1–N2 80.8(1)°; N1–Cu1–N3^{i} 122.6(1)°; N1–Cu1–N4^{i} 139.5(1)°; N2–Cu1–N3^{i} 127.7(1)°; N2–Cu1–N4^{i} 111.9(1)°; N3^{i}–Cu1–N4^{i} 81.1(1)°. Symmetry codes: (i) $-x+1, y, -z+3/2$.

anions do not interact with Cu^{I}. One water molecule is also present. In the $[Cu_2\mathbf{L}_2]^{2+}$ molecular cation, each Cu^{I} is coordinated by four nitrogens, two belonging to one ImQ half of an **L** ligand and two belonging to an ImQ half of the second **L** ligand. The two **L** ligands intertwine to give a double helix.

The $[Cu_2\mathbf{L}_2]$ molecular cation is characterized by a pseudo-orthorhombic symmetry. The two Cu^{I} ions and the two **L** ligands are symmetrical for the crystallographic twofold axis parallel to the *b* direction, so that the half of the formula unit comprises the asymmetric unit; two pseudo-C_2 axes, normal to the crystallographic one and thus forming a triad of orthogonal twofold rotation axes as in orthorhombic symmetry, can also be defined. In particular, one pseudo-C_2 axis, parallel to the *a** crystallographic direction, allows the superimposition of each half of a single **L** ligand over the other half of that ligand with a 180° rotation. The two halves of each **L** ligand can then be considered almost symmetrical for this pseudo-symmetry element; deviations can be found for some atoms in the quinoline rings. Anyway, the loss of symmetry of the crystal from orthorhombic to monoclinic is essentially due to the $CF_3SO_3^-$ anions, which cannot be related to a twofold rotation axis. The coordination around each Cu^{I} cation can be described as distorted tetrahedral with Cu–N bond lengths ranging from 2.016(3) Å and 2.097(3) Å. The distance between the two Cu^{I} ions is 3.669(1) Å. The crystal is maintained by van der Waals forces and weak interactions involving the water molecule.

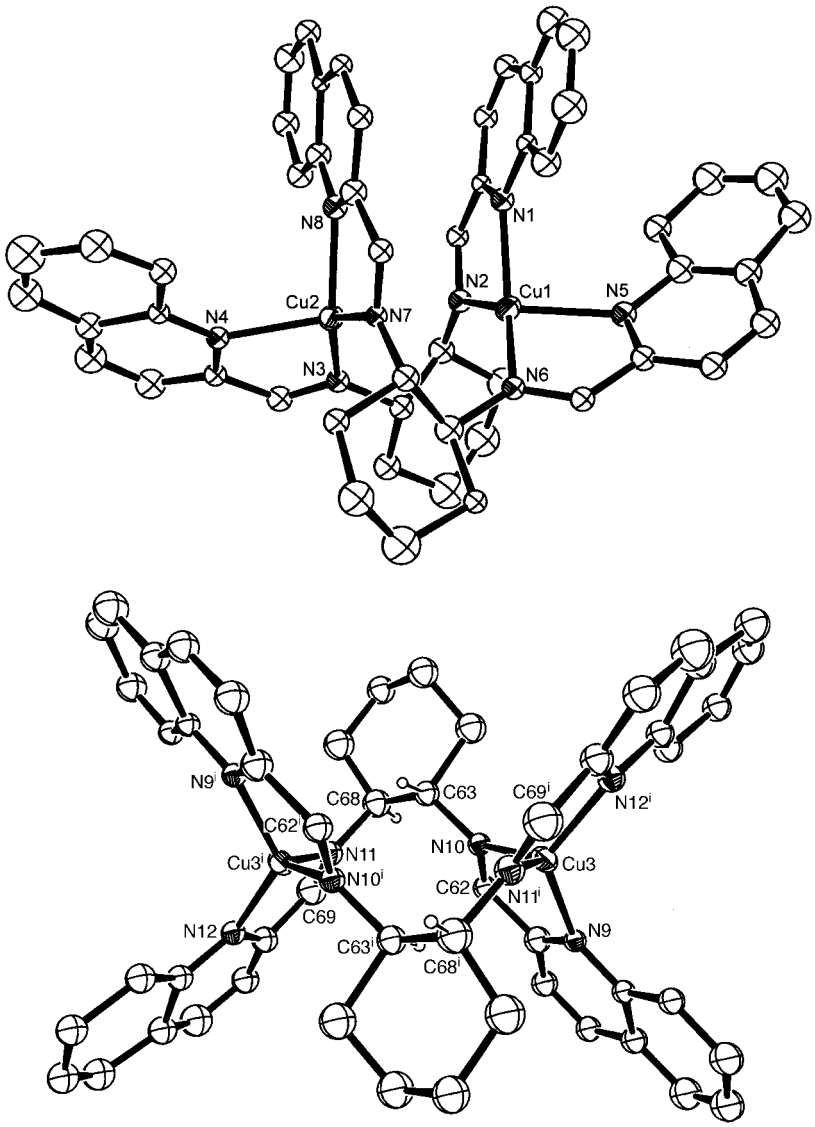

Figure 3. Top: ORTEP view of $[Cu^{I}_2\mathbf{L}_2](ClO_4)_2$ in the helical conformation. C atoms were not numbered for sake of clarity. Displacement parameters are drawn at 20% probability level. Selected bond lengths: Cu1–N1 2.080(26) Å; Cu1–N2 2.000(26) Å; Cu1–N5 2.168(27) Å; Cu1–N6 2.051(24) Å; Cu2–N3 2.024(26) Å; Cu2–N4 2.173(25) Å; Cu2–N7 2.016(23) Å; Cu2–N8 2.105(26) Å. Selected bond angles: N1–Cu1–N2 82(1)°; N1–Cu1–N5 96(1)°; N1–Cu1–N6 138(1)°; N2–Cu1–N5 82(1)°; N2–Cu1–N6 134(1)°; N5–Cu1–N6 82(1)°; N3–Cu2–N4 81(1)°; N3–Cu2–N7 135(1)°; N3–Cu2–N8 135(1)°; N4–Cu2–N7 121(1)°; N4–Cu2–N8 103(1)°; N7–Cu2–N8 82(1)°. Bottom: ORTEP view of the nonhelical (boxlike) $[Cu^{I}_2\mathbf{L}_2](ClO_4)_2$. C atoms were not numbered for sake of clarity. Displacement parameters are drawn at 20% probability level. Selected bond lengths: Cu3–N9 2.014(26) Å; Cu3–N10 1.999(25) Å; Cu3–N11^{i} 1.985(28) Å; Cu3–N12^{i} 2.022(26) Å. Selected bond angles: N9–Cu3–N10 84(1)°; N9–Cu3–N11^{i} 122(1)°; N9–Cu3–N12^{i} 128(1)°; N10–Cu3–N11^{i} 124(1)°; N10–Cu3–N12^{i} 126(1)°; N11^{i}–Cu3–N12^{i} 80(1)°. Symmetry codes: (i) $-x, -y, -z+1$.

$[Cu^{I}_2\mathbf{L}_2](ClO_4)_2$: The crystal structure of this compound revealed some unusual features. Two different forms of the $[Cu^{I}_2\mathbf{L}_2]$ molecular cation coexist in the crystal, one with a helical-type structure (Figure 3, top) and the other with a boxlike (i.e., nonhelical) structure (Figure 3, bottom). The two species are present in the crystal in a 2:1 ratio (helix:box). Each unit cell contains four helical molecular cations, two boxlike cations, six perchlorate anions and six water molecules. The nonhelical molecular cation has a crystallographic centre of symmetry in the midpoint between Cu3 and Cu3^{i}, so that only half of this molecule is defined in the asymmetric unit.

It is of striking interest for the discussion of the solution behaviour of Cu^{I} complexes with **L** to note that in the helical molecular cations found with ClO_4^- as the anion, there is a certain degree of asymmetry due to the reciprocal positioning of the ligands. Only one pseudo-C_2 axis, which lies normal to the *c* crystallographic direction, can in fact be defined for the helical complex and allows each single **L** ligand to superimpose on the other. No symmetry elements relate the two

  0947-6539/99/0512-3682 $ 17.50+.50/0 *Chem. Eur. J.* **1999**, *5*, No. 12

halves *of the same ligand*, which therefore are not equivalent. In particular, in this molecular cation two quinoline rings that belong to two different **L** ligands are almost parallel, with an angle of 10.8° and distances ranging from 3.2 to 3.8 Å.

Each Cu^{I} cation, both in the helical and in the boxlike structures, is coordinated by four nitrogen atoms, two belonging to one ImQ half of a **L** ligand and two belonging to an ImQ half of the second **L** ligand. The coordination can be described as distorted tetrahedral. In the helical form some unusually long Cu–N bond lengths were found [Cu1–N5 2.168(27) Å; Cu2–N4 2.173(25) Å]. It is worth noting that the Cu–Cu distance is much larger in the boxlike molecular cation (Cu3–$Cu3^{i}$ 4.906 Å) than in the helical structure (Cu1–Cu2 3.322 Å).

$[Cu^{II}L]^{2+}$ and $[Cu^{I}_{2}L_{2}]^{2+}$ molecular cations in solution: As already mentioned in the synthesis section above, addition of substoichiometric quantities of $Cu(CF_3SO_3)_2$ to **L** in an acetonitrile solution was followed by UV/Vis spectroscopy. Clear isosbestic points (270 and 305 nm) were found which indicates that a single species was formed, while plotting absorbance (at any wavelength) versus equivalents of added Cu^{II} gave titration profiles that reached a maximum at one equivalent and continued with a plateau till the end of the titration (3 equiv). The colour of the solution (green) and the band position and intensity (336 nm, $\varepsilon = 12000\ mol^{-1}\ 1cm^{-1}$; 668 nm, $\varepsilon = 105\ mol^{-1}Lcm^{-1}$) fits well with what found in the literature for distorted square planar Cu^{II} complexes with ligands featuring only sp^2 nitrogen donors: with functionalized quaterpyridine ligands, charge transfer (CT) and d–d bands at 314 nm ($\varepsilon = 12200\ mol^{-1}Lcm^{-1}$) and at 625 nm ($\varepsilon = 270\ mol^{-1}Lcm^{-1}$), respectively[9] or at 324 nm ($\varepsilon = 35200\ mol^{-1}Lcm^{-1}$) and 626 nm ($\varepsilon = 270\ mol^{-1}Lcm^{-1}$), respectively,[8a] have been reported. Moreover, authentic crystalline $[Cu^{II}L](CF_3SO_3)_2$, that belonged to the same batch from which crystals for X-ray diffraction were taken, when dissolved in acetonitrile gave a spectrum that could be superimposed over the final spectrum obtained in the spectrophotometric titration experiments. On this basis, one can reasonably say that in acetonitrile solution Cu^{II} is coordinated by a single **L** ligand with square planar coordination.

In the case of the Cu^{I} complexes, a family of spectra with two isosbestic points (265 and 298 nm) and a growing band centred at 536 nm ($\varepsilon = 3500\ mol^{-1}Lcm^{-1}$; a shoulder can also be identified at 470 nm) was again observed during titration experiments (addition of substoichiometric quantities of $[Cu(CH_3CN)_4]ClO_4$ to an acetonitrile solution of **L**). Superimposable spectra were recorded on further additions after one equivalent of metal salt was reached, so that titration profiles (A vs. equiv. of Cu^{I} at any wavelength) reached a maxiumum and then changed sharply into a plateau at one equivalent. The wavelength maximum and the purple-brown colour of the solution are typical of the MLCT band for tetrahedral complexes of Cu^{I} with bidentate ligands containing sp^2 nitrogen atoms as donors: in the case of dimeric helical complexes with linear quaterpyridine ligands, absorption maxima have been reported at 550 nm ($\varepsilon = 4940\ mol^{-1}Lcm^{-1}$)[8a] and at 454 nm ($\varepsilon = 2717\ mol^{-1}Lcm^{-1}$),[9] but a variety of λ_{max} positions and band intensities may be expected even with the same ligand on changing substituents on its backbone (e.g., λ_{max} and ε are in the range 435–479 nm and $3620–14200\ mol^{-1}Lcm^{-1}$ for a series of substituted $[Cu^{I}(phenanthroline)_2]^{+}$ complexes[12]). The spectrum recorded at one equivalent (or more) of added metal could be superimposed over that measured on solutions obtained from authenthic crystalline samples of either $[Cu^{I}_{2}L_{2}](CF_3SO_3)_2$ or $[Cu^{I}_{2}L_{2}](ClO_4)_2$. Moreover, mass spectra (ESI) recorded on solutions obtained by either dissolving the crytalline products or by in situ reaction of **L** with one equivalent of $[Cu(CH_3CN)_4]ClO_4$ gave further proof of the existence, in acetonitrile, of the $[Cu^{I}_{2}L_{2}]^{2+}$ species (vide supra).

While this data demonstrated that, also in solution, a dimeric $[Cu^{I}_{2}L_{2}]^{2+}$ species exists, X-ray diffraction studies showed that two different helical structures and one nonhelical dimer can be found in the solid state (in particular, one nonhelical and one helical dimer coexist in the same crystal cell!), depending on the chosen anion. In order to gain some more insight on what really exists in CH_3CN, ^1H NMR spectra were measured in CD_3CN i) on the free ligand **L**, ii) on crystalline $[Cu^{I}_{2}L_{2}](CF_3SO_3)_2$, iii) on crystalline $[Cu^{I}_{2}L_{2}](ClO_4)_2$ and iv) after in situ reaction of **L** and $[Cu(CH_3CN)_4]ClO_4$ (1:1). The results showed that the spectra recorded for the three metal-containing solutions were identical. This indicates that the same species (or the same composition of an equilibrium mixture of two species, vide infra) exists in solution, independently upon the chemical history of the solution and the counter anion. In particular, if the aromatic zone of the NMR spectra is taken into consideration (the aliphatic protons zone is strongly affected by the presence of residual CH_3CN in the deuterated solvent), for $[Cu^{I}_{2}L_{2}]^{2+}$ a set of signals prevails that features the same number and type of signals obtained for free **L** (Figure 4), although peaks are shifted and distributed on a larger range ($\delta = 7.5–8.35$ and 6.9–8.6 for **L** and $[Cu^{I}_{2}L_{2}]^{2+}$, respectively).

Moreover, a second, much less intense series of signals is found for the metal-containing solutions; this, unfortunately, is for the most part hidden under the main sequence peaks, so that only two singlets ($\delta = 8.89$ and 9.18, same area), two doublets ($\delta = 7.91$ and 7.95, same area) and two triplets ($\delta =$ 7.50 and 7.60, same area) can be clearly seen. This points towards the existence of only one main species in acetonitrile solution (with a second one existing only in a small percentage, vide infra), but on the basis of these data, it cannot be said if it is of the helical or nonhelical kind. As a matter of fact, both the helical structure found for $[Cu^{I}_{2}L_{2}](CF_3SO_4)_2$ (Figure 2) and the nonhelical dimer contained in the cell of $[Cu^{I}_{2}L_{2}](ClO_4)_2$ (Figure 3, bottom) could display such a spectrum: both structures have symmetry such that not only is each ligand equivalent to the other, but also each half of one ligand is equivalent to the other half of the same ligand. Their NMR spectra should then display only a shift in the signals with respect to the free ligand **L**. However, an indication of the nature of this symmetric species existing in solution can be obtained by comparing the crystal structures (symmetric double helix and nonhelical dimer) with the NMR signals of the two hydrogens bound to the cyclohexyl carbons bearing the imine nitrogen atoms (C11

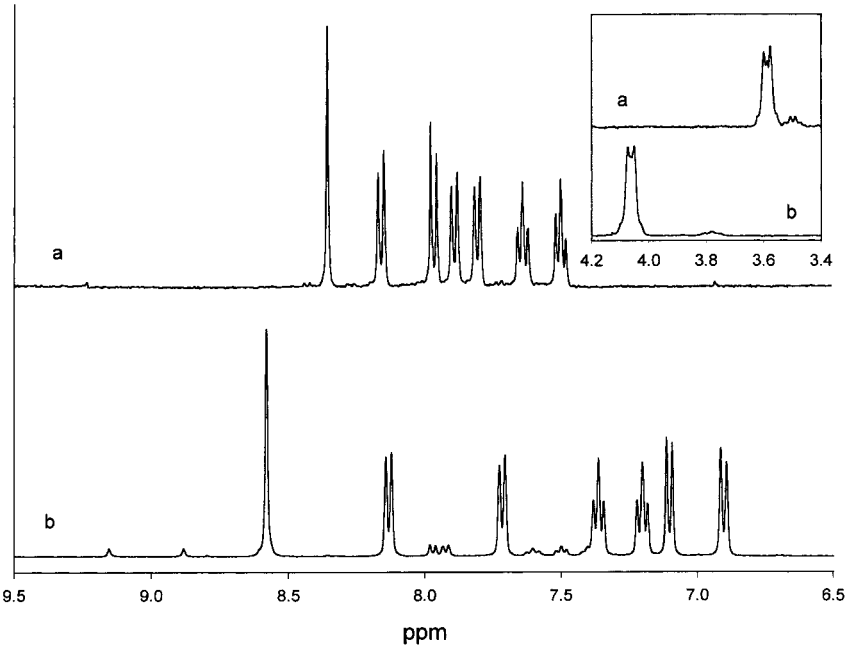

Figure 4. ^{1}H NMR spectra (aromatic part) of a) ligand **L** and b) the $[Cu_2\mathbf{L}_2]^{2+}$ cation with CD_3CN as solvent. In the inset is reported the spectrum portion relative to the C**H**(N) protons of the cyclohexane ring for a) the free ligand and b) the complex cation.

and C16 in Figure 2 and C63 and C68 in Figure 3, bottom). In the crystal structure of the symmetric helical complex, the two hydrogens, which are evidently *trans* to each other, lie in an almost identical environment. According to the calculated positions of the hydrogens, the C11−H and C16−H bonds forms comparable angles (48.9° and 54.2°) with respect to the plane defined by C11−N2=C10 and by C16−N3=C17, respectively (Figure 2), so they are both close to the C=N double bond and to its shielding cone. On the other hand, from the structure of the nonhelical dimer (Figure 3, bottom), it can be seen that the two corresponding hydrogens lie in different surroundings with respect to each other: the C63−H and C68−H bonds form angles of 139.5° and 22.4° with respect to the plane defined by C63−N10=C62 and by C68−N11=C69, respectively, so that one hydrogen (that on C68) is close to the C=N double bond and its shielding cone, whereas the other (that on C63) is opposite to it. This latter case should result in a significant split, in the NMR spectrum, of the signals that relate to the two hydrogens, while in the former case, one should expect the two signals to be found at very close chemical shift. As a matter of fact, only one multiplet is found in the spectra for the C**H**−C=N hydrogens, with the same shape as those in the free ligand, but is shifted with respect to the free ligand ($\Delta\delta = 0.55$, see Figure 4, inset). This points towards the helical structure found for $[Cu^I_2\mathbf{L}_2](CF_3SO_3)_2$ as being the species that prevails in CH_3CN solution.

The helical molecular cations found in the cell of $[Cu^I_2\mathbf{L}_2](ClO_4)_2$ have a lower degree of symmetry, with respect to that of $[Cu^I_2\mathbf{L}_2](CF_3SO_3)_2$ and the nonhelical dimer of $[Cu^I_2\mathbf{L}_2](ClO_4)_2$. While the two ligands are equivalent with respect to each other, the two halves of the same **L** are no longer equivalent (see Figure 3, top): one ImQ half faces another one that belongs to the second **L** ligand, while the other half is isolated. According to this, one should expect the signals, at least those of the aromatic protons, to split into two sets of identical intensity. Indeed, this is what is observed for the series of signals of low intensity found in the ^{1}H NMR spectrum of $[Cu^I_2\mathbf{L}_2]^{2+}$. In particular, the twin singlets found at $\delta = 8.89$ and 9.18 can be reasonably assigned to the −N=CH− protons of the "asymmetric helix", and the sum of their area can be compared with the area of the main signal for −N=CH− ($\delta =$ 8.58) to evaluate the composition of the solution under the conditions of the measured spectrum (20 °C). A value of 13 % is obtained for the asymmetric helix and 87 % for the symmetric one. Moreover, a series of spectra has been recorded on a CD_3CN solution of $[Cu^I_2\mathbf{L}_2](CF_3SO_3)_2$, in the 303–250 K temperature range. Comparison of the areas of the −N=CH− singlets revealed that on lowering temperature the percent of the asymmetric helix slightly decreases, reaching a minimum of 8 % at 250 K; this indicates that there is only a small difference in energy between the two forms. Energetics can be evaluated in more detail from the ln$K$ versus $1/T$ plot for the equilibrium symmetric helix ⇌ asymmetric helix (with $K =$ [% asymmetric helix]/[% symmetric helix]). The following values were calculated: $\Delta H^{\ominus} = 1.75$ kcal mol^{-1}; $T\Delta S^{\ominus} = 0.65$ kcal mol^{-1} (at 20 °C). Finally, on raising the temperature to 303 K, a spectrum with a much lower resolution of both sets of signals was observed; this broadening is probably due to the faster exchange between the symmetric and asymmetric forms. The equilibrium between the two forms is slow for the timescale of the NMR experiments, at least when temperature is maintained at 20 °C or lower, but, significantly, few seconds (i.e., the time necessary to prepare an NMR or UV/Vis sample) are sufficient for any 1:1 mixture of **L** and Cu^I to reach, in solution, the same equilibrium composition, independent of the counter anion or the chemical history of the dissolved complex.[13] In this regard, it is important to note that the recorded spectra do not change with time, as shown by NMR measurements carried out at 20 °C for 6 hours (30 minutes intervals) on solutions obtained either from crystalline products or by in situ complexation.

Electrochemical switching between $[Cu^I_2\mathbf{L}_2]^{2+}$ and $[Cu^{II}\mathbf{L}]^{2+}$: Cyclic voltammetry experiments in acetonitrile solution were performed on $[Cu^I_2\mathbf{L}_2](CF_3SO_3)_2$ and $[Cu^{II}\mathbf{L}](CF_3SO_3)_2$. In both cases, the same profile was found in the $1500 < E < -300$ mV (vs. SCE) range, featuring an irreversible oxidation wave at 985 mV versus SCE, with no return peak, and an irrevesible reduction peak at 440 mV versus SCE, again with no return peak (Figure 5).

0947-6539/99/0512-3684 $ 17.50+.50/0 *Chem. Eur. J.* **1999**, *5*, No. 12

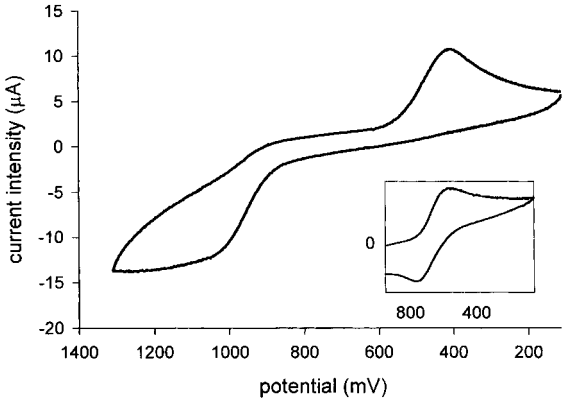

Figure 5. Cyclic voltammetry profile for $[Cu_2^{I}\mathbf{L}_2]^{2+}$ or $[Cu^{II}\mathbf{L}]^{2+}$, in CH_3CN, 0.1M in (tBu)$NClO_4$. Potential scale vs. SCE. Inset displays the CV profile for the $Cu^{I}/\mathbf{L}'$ 1:2 complex.

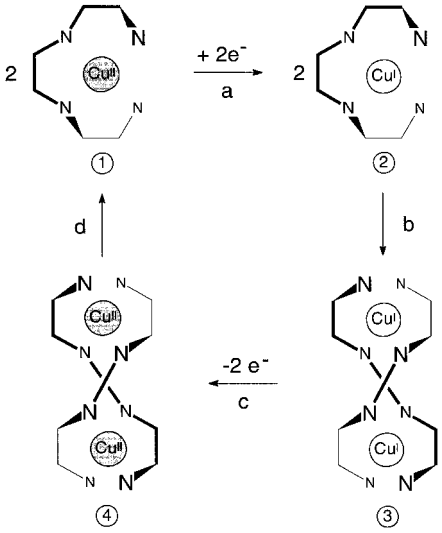

Figure 6. The square scheme underlying the assembly/disassembly process in the $Cu^{II}/Cu^{I}/L$ system. The cyclic process can be initiated either from the monomeric complex **1** or from the dimeric helical complex **3**. The transient species **2** and **4** have lifetimes less than 250 ms, as estimated from cyclic voltammetry experiments.

Significantly, in a solution of $[Cu_2^{I}\mathbf{L}_2](CF_3SO_3)_2$ if the oxidation scan is reversed before the irreversible oxidation peak (for example at 800 mV vs. SCE), no signal is observed on the reduction scan. Vice versa, in a solution containing $[Cu^{II}\mathbf{L}](CF_3SO_3)_2$ no peaks are observed in oxidation, if the reduction scan is reversed before the potential of the irreversible reduction peak (for example at 600 mV).

This can be compared with what is found for the complexes with ligand $\mathbf{L}'$, which were prepared in situ, either with Cu^{II} or Cu^{I}, immediately before the electrochemical experiments.[14] In both cases, a CV profile displaying a reversible one electron wave was observed, with $E_{1/2} = 710$ mV (Cu^{I}, $\Delta E = 130$ mV) and 715 mV (Cu^{II}, $\Delta E = 110$ mV) versus SCE (see inset in Figure 5 for the latter case). This potential is not uncommon for the $Cu^{II/I}$ couple in 2:1 complexes with bidentate sp^2 nitrogen ligands,[15] while the large ΔE values indicate a partial irreversibility due to the rearrangement from a planar or distorted octahedral coordination, typical of Cu^{II}, to a tetrahedral one during the reduction process (or vice versa).

The CV profile observed for the $Cu^{II}/Cu^{I}/\mathbf{L}$ system (Figure 5), compared with that pertinent to the $Cu^{II}/Cu^{I}/\mathbf{L}'$ reference system (Figure 5, inset) can be accounted for on the basis of the square scheme reported in Figure 6. Moving from the upper left corner of the scheme, the $[Cu^{II}\mathbf{L}]^{2+}$ complex (**1**) is reduced to the $[Cu^{I}\mathbf{L}]^{+}$ monomeric transient (**2**), which self-assembles to give the dimeric helical species $[Cu_2^{I}\mathbf{L}_2]^{2+}$ (**3**). Even by carrying out CV experiments at the fastest potential scan rate (2.0 $V s^{-1}$) along the 550–300 mV potential range, no return peak was observed. This indicates that the lifetime of the Cu^{I} monomeric transient **2** is lower than 250 ms. Then, on oxidation of the stable complex **3**, the helical $[Cu_2^{II}\mathbf{L}_2]^{4+}$ transient (**4**) must form, which immediately disassembles to give two square planar complexes of **1**, thus completing the cycle. Also in this process, no return peak was observed on the fastest available potential scan rate, over the 800–1090 mV potential range, indicating for the dimeric Cu^{II} transient **4** a lifetime lower than 250 ms. It is worth noting that the development of the process and the CV response are independent on the starting corner of the scheme, whether the upper left (species **1**) or lower right (species **3**).

The occurrence of the electrochemically triggered assembling/disassembling process can be visually perceived and further characterized by means of exhaustive electrolysis experiments and coupled spectrophotometric–coulometric experiments. Controlled potential coulometry (CPC) experiments were performed in a cell in which a quartz fiber optic probe was dipped; this was connected to a diode-array spectrophotometer, thus allowing us to monitor the species present in solution during the whole process. Green solutions containing $[Cu^{II}\mathbf{L}]^{2+}$ can be reduced by setting the platinum gauze, which acts as a working electrode, to a potential of 350 mV versus SCE or lower. While the reduction proceeded, a family of spectra was recorded (see Figure 7), which display two isosbestic points (at 320 and 382 nm) and in which the

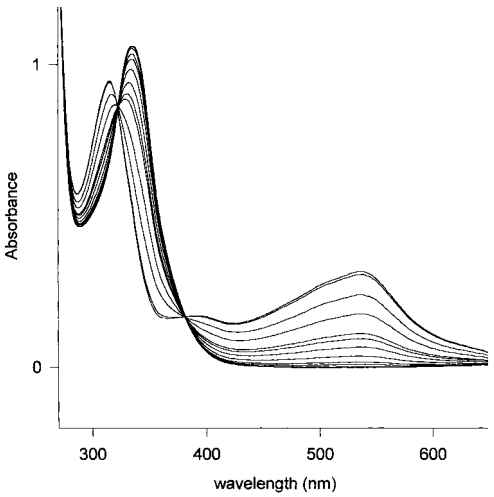

Figure 7. Spectra recorded in the electrochemical cell during a controlled potential coulometry experiment: $[Cu^{II}\mathbf{L}]^{2+}$ is reduced to $[Cu_2^{I}\mathbf{L}_2]^{2+}$, at a potential of 350 mV vs. SCE. The band at 336 nm decreases in intensity, while that at 536 nm increases. Superimposable spectra are obtained after about 20 minutes. The electric charge measured by coulometry corresponds to 1 e^- per Cu^{II} centre.

bands of the Cu^{II} species ($\lambda = 336$ and 668 nm) decrease in intensity and that of the $[Cu^{I}_2\mathbf{L}_2]^{2+}$ chromophore increase ($\lambda = 536$ nm).

Superimposable spectra, identical to that of authentic $[Cu^{I}_2\mathbf{L}_2](CF_3SO_3)_2$, were found after the passage of one mole of electrons per mole of $[Cu^{II}\mathbf{L}](CF_3SO_3)_2$, this took 20 minutes under the employed experimental conditions (concentrations: 10^{-4} mol L^{-1}; electrolysed volume: 70 mL). The obtained purple-brown solution of $[Cu^{I}_2\mathbf{L}_2](CF_3SO_3)_2$ was then re-oxidized by setting the working electrode at a potential of 1020 mV versus SCE. The same isosbestic points were found, the band at 536 nm decreased and those at 336 and 668 increased, reaching a final spectrum in 20 minutes (after the passage of 2 moles of electrons per mole of $[Cu^{I}_2\mathbf{L}_2]^{2+}$); this spectrum was exactly superimposable with the starting spectrum obtained when solid $[Cu^{II}\mathbf{L}](CF_3SO_3)_2$ was dissolved. Significantly, the reduction/oxidation, that is, assembly/disassembly process, was carried out up to ten times without significant modifications of the final spectra; this gives an indication of the true bistability of the system and high reversibility of the electrochemically driven process (the same results were found starting from a solution of solid $[Cu^{I}_2\mathbf{L}_2](CF_3SO_3)_2$ instead of $[Cu^{II}\mathbf{L}](CF_3SO_3)_2$).

Conclusion

The assembly/disassembly of helicate metal complexes is one of the more fascinating processes so far observed in supramolecular solution chemistry.[4] The stereochemical preferences of the metal ion used as a template and the denticity of the coordinating subunits of the ligand determine the multiplicity of the helix, whether double or triple. In particular, metal centres imposing a tetrahedral coordination geometry (d^{10} cations: e.g., Cu^{I}, Ag^{I}, Zn^{II}) and ligands containing bidentate subunits give rise to double helicates, an example of which is described in the present work. Cu^{I} is unique, as it possesses a stable adjacent oxidation state, Cu^{II}, which strongly prefers square planar coordination, a stereochemical arrangement hardly suitable for helix formation. Thus, $Cu^{I}-Cu^{II}$ oxidation induces the disassembly of the helix, a process which can be reversed through $Cu^{II}-Cu^{I}$ reduction; this provides an example of an oriented molecular motion, which can be controlled by an external input, that is, the variation of the redox potential. Electrochemistry, in particular the CV technique, offers a powerful tool to investigate both thermodynamic and kinetic aspects associated to the formation of Cu^{I} helicates. In particular, the potential of the irreversible oxidation peak in the CV profile (when compared with the $E_{1/2}$ value observed for the mononuclear model complex, Figure 5, as an example) provides information on the stability of the $[Cu^{I}_2\mathbf{L}_2]^{2+}$ helicate and on its resistance towards disassembly and formation of $2[Cu^{II}]\mathbf{L}^{2+}$. On the other hand, the appearance or nonappearance of the return peak in CV experiments at high potential scan rate may give a direct insight on the velocity of helix formation and destruction. In this respect, imine-quinoline ligands like those described in this work appear especially convenient and versatile: in particular, the steric and electronic features of the ligand (length and rigidity of the di-imine spacer, hindering substituents, presence on the heterocyclic ring of electron donating/withdrawing groups, etc.) can be extensively modified through the choice of the appropriate fragments to be connected by the Schiff base condensation. This allows us to investigate in detail how these structural factors affect the thermodynamic and kinetic stability of Cu^{I} helicates. Studies in this direction are currently under way in our laboratory.

Experimental Section

Syntheses: All the starting materials were purchased from Aldrich and used without further purification. No significant differences were found in the composition or purity of the products when the syntheses were performed under an inert atmosphere (N_2) instead of in air. Mass spectra (ESI) were recorded on a Finnigan MAT TSQ 700 instrument, NMR spectra on a Bruker AMX 400 spectrometer, and IR spectra on a Mattson 5000 FT-IR instrument.

Bis-*N*,*N*′-(2-methylquinoline)-1,2-*trans*-cyclohexanediimine (L): A solution of 2-quinoline carboxyaldehyde (1 g, 6.36 mmol) in CH_2Cl_2 (30 mL) was added dropwise, at room temperature, to a solution of *trans*-1,2-diamino cyclohexane (0.36 g, 3.18 mmol) in CH_2Cl_2 (50 mL), in which anhydrous Na_2SO_4 (0.5 g) was already suspended in order to remove the water produced by the Schiff condensation. After 18 hours, the mixture was filtered, and the solvent removed on a rotary evaporator to obtain a yellowish solution (5 mL volume), from which the product precipitated in 24 hours as a white–yellow solid. **L** was collected by suction filtration, washed with *n*-hexane (2×5 mL) and dried in a vacuum dessicator (85% yield). $C_{26}H_{24}N_4$ (392.40): calcd C 79.61, H 6.12, N 14.27; found C 79.60, H 6.10, N 14.15%; IR (NaCl cells, nujol mull): $\tilde{\nu} = 1643$ (sharp, imine C=N stretch), 1593 cm^{-1} (sharp, C=N stretch in the quinoline ring); NMR (CD_3CN): $\delta = 8.35$ (s, 2H; −N=CH−), 8.18 (d, 2H), 7.98 (d, 2H), 7.80 (d, 2H), 7.63 (dt, 2H), 7.50 (dt, 2H) [Hs of the quinoline rings], 3.60 (m, 2H; CH(N)−CH(N) of the cyclohexane ring), 1.2–2.0 (m; CH_2 of the cyclohexane ring, CH_3CN solvent impurity).

***N*-(2-Methylquinoline)-cyclohexylimine (L′)**: A solution of 2-quinolinecarboxyaldehyde (2 g, 12.7 mmol) in CH_2Cl_2 (30 mL) was added dropwise to a solution of cyclohexylamine (1.26 g, 12.7 mmol) in CH_2Cl_2 (50 mL), in which anhydrous Na_2SO_4 (1.0 g) was already suspended. After 16 h stirring at room temperature, the mixture was filtered and the obtained solution evaporated to dryness on a rotary evaporator. A semisolid was obtained, which was washed with *n*-hexane (5×2 mL) and diethylether (5×2 mL) and dried under vacuum to give pure **L′** (90% yield). IR (NaCl cells, pure substance): $\tilde{\nu} = 1645$ (sharp, imine C=N stretch), 1597 cm^{-1} (sharp, C=N stretch in the quinoline ring); NMR (CD_3CN): $\delta = 8.55$ (s, 1H; −N=CH−), 8.33 (d, 1H), 8.12 (m, 2H), 7.98 (d, 1H), 7.81 (dt, 1H), 7.66 (dt, 1H) [Hs of the quinoline ring], 3.45 (m, 1H; CH−N=CH−), 1.3–2.2 (m, CH_2 of the cyclohexane ring, CH_3CN solvent impurity).

$[Cu^{II}\mathbf{L}](CF_3SO_3)_2$: Ligand **L** (0.50 g, 1.27 mmol) was dissolved in CH_3CN (20 mL) and treated with a solution of anhydrous $Cu(CF_3SO_3)_2$ (0.46 g, 1.27 mmol) in CH_3CN (5 mL). The solution immediately turned deep green and after stirring for 0.5 h it was left to stand. After 20 h $[Cu^{II}\mathbf{L}](CF_3SO_3)_2$ was obtained as dark green crystals, which were collected by suction filtration, dried under vacuum in a dessicator and found suitable for single-crystal X-ray diffraction analysis. Yield: 59%; $C_{28}H_{24}CuF_6N_4O_6S_2$ (754.18): calcd C 44.61, H 3.18, N 7.43; found C 44.51, H 3.13, N 7.48%; IR (NaCl, nujol mull): $\tilde{\nu} = 1675$ (sharp, imine C=N stretch), 1591 cm^{-1} (sharp, C=N of the quinoline system).

$[Cu^{I}_2\mathbf{L}_2](CF_3SO_3)_2 \cdot H_2O$: Ligand **L** (0.50 g, 1.27 mmol) was dissolved in CH_3OH (30 mL) that contained $NaCF_3SO_3$ (0.86 g, 5 mmol) and was treated with a solution of $[Cu(CH_3CN)_4]ClO_4$ (0.42 g, 1.27 mmol) in CH_3OH (5 mL). The solution immediately turned deep purple. After 2 h, black-purple microcrystals of the product formed, which were collected by suction filtration, dried in a dessicator under vacuum, redissolved in acetonitrile and crystallized by slow diffusion of diethyl ether. The obtained crystals were found suitable for X-ray diffraction studies. Yield 40%; $C_{54}H_{50}Cu_2F_6N_8O_7S_2$ (1228.25): calcd C 52.83, H 4.07, N 9.12; found C 52.90,

0947-6539/99/0512-3686 $ 17.50+.50/0 *Chem. Eur. J.* **1999**, *5*, No. 12

H 4.05, N 9.11; IR (NaCl, nujol mull): $\tilde{\nu} = 1665$ (sharp, imine C=N stretch), 1592 cm^{-1} (sharp, C=N stretch of the quinoline system).

$[Cu^{I}_2L_2](ClO_4)_2 \cdot H_2O$: Ligand **L** (0.50 g, 1.27 mmol) was dissolved in CH_3CN (20 mL) and treated with a solution of $[Cu(CH_3CN)_4]ClO_4$ (0.42 g, 1.27 mmol) in CH_3CN (5 mL). Slow evaporation of the deep purple solution gave the product as black-purple crystals, which were collected by suction filtration, dried under vacuum and found suitable for X-ray diffraction studies. Yield 52 %; $C_{52}H_{50}Cl_2Cu_2N_8O_9$: calcd C 55.34, H 4.43, N 9.92 %; found C 55.30, H 4.42, N 9.92 %; IR (NaCl, nujol mull): $\tilde{\nu} = 1664$ (sharp, imine C=N stretch), 1593 cm^{-1} (sharp, C=N of the quinoline system).

Spectrophotometric titrations: UV/Vis spectra were recorded on a Hewlett–Packard 8453 diode array spectrophotometer. Titrations were performed on 20–30 mL samples of solutions (10^{-4} mol L^{-1}) of ligand in CH_3CN, by microadditions of a CH_3CN solution of either $[Cu^{I}(CH_3CN)_4]ClO_4$ or $Cu(CF_3SO_3)_2$. In a typical experiment, metal salt (1 equiv) was added in 20 portions from the metal salt solution (10 μL).

Electrochemistry and spectroelectrochemistry: Electrochemical measurements (cyclic voltammetry, CV, and controlled potential coulometry, CPC) were performed with a P.A.R. 273 potentiostat/galvanostat, under the control of a PC, with dedicated software. In CV studies (CH_3CN solution, 0.1 mol L^{-1} $(tBu)_4NClO_4$), the working electrode was a platinum microsphere and the counter electrode a platinum foil. A platinum wire was used as a pseudo reference electrode and was calibrated versus ferrocene as an internal standard. The measured potentials were then referred to SCE ($E_{1/2}$ for the Fc^+/Fc couple: 425 mV vs. SCE, in CH_3CN[16]). CPC experiments were performed on solutions of $[Cu^{I}_2L_2](CF_3SO_3)_2$ or $[Cu^{II}L](CF_3SO_3)_2$ (5×10^{-5}–10^{-4} mol L^{-1}), with a platinum gauze as a working electrode. The counter-electrode compartment was separated from the working compartment by a U-shaped bridge, filled with CH_3CN (0.1 mol L^{-1}) in $(tBu)_4NClO_4$. The reference electrode, a platinum wire dipped in the working cell, was calibrated through CV experiments prior to CPC. The spectra of the solutions in the working cell were taken during the electrolysis by using a quartz fiber optic probe (Hellma, 661.500 QX) connected to the diode-array spectrophotometer, with an optical path of 20 mm.

X-ray data collection and processing: Crystal data and details on the crystallographic study are reported in Table 1. For crystals $[Cu^{II}L](CF_3SO_3)_2$ and $[Cu^{I}_2L_2](CF_3SO_3)_2$, unit cell parameters and intensity data were obtained on an Enraf–Nonius CAD-4 four-circle diffractometer, located at Centro Grandi Strumenti, Pavia. The cell dimensions were obtained by least-squares fitting of 25 centered reflections monitored in the ranges $5.32^\circ < \theta < 12.54^\circ$ and $8.58^\circ < \theta < 13.22^\circ$, respectively. For crystal $[Cu^{I}_2L_2](ClO_4)_2$, diffracted intensities were collected on a Philips PW 1100 four-circle diffractometer. Unit cell parameters were obtained by an accurate procedure based on the Philips LAT routine[17] and confirmed on an Enraf-Nonius FAST area-detector diffractometer by monitoring ≈120 reflections in the range $5^\circ < \theta < 20^\circ$.

Crystals $[Cu^{I}_2L_2](ClO_4)_2$ and $[Cu^{II}L](CF_3SO_3)_2$ showed very low diffraction and data collections were performed over a restricted range of θ (2–20° and 2–25°, respectively). No improvement to the resolution of the models would in fact have been obtained by increasing the theta range because most of the reflections would have been weak; on the contrary, a set of equivalent reflections was collected for a better determination of the measured data. In both cases the number of observed reflections/number of parameters ratios were quite low. Anyway no chemically unacceptable bond length or angle was found and the final difference Fourier maps were

Table 1. Crystallographic data for the compounds $[Cu^{II}L](CF_3SO_3)_2$, $[Cu^{I}_2L_2](CF_3SO_3)_2 \cdot H_2O$ and $[Cu^{I}_2L_2](ClO4)_2 \cdot H_2O$.

	$[Cu^{II}L](CF_3SO_3)_2$	$[Cu^{I}_2L_2](CF_3SO_3)_2 \cdot H_2O$	$[Cu^{I}_2L_2](ClO4)_2 \cdot H_2O$
formula	$C_{28}H_{24}CuF_6N_4O_6S_2$	$C_{54}H_{50}Cu_2F_6N_8O_7S_2$	$C_{52}H_{50}Cl_2Cu_2N_8O_9$
molecular weight	754.17	1228.24	1129.01
colour	green	black	black
size [mm]	0.18 × 0.22 × 0.29	0.29 × 0.43 × 0.58	0.13 × 0.19 × 0.19
crystal system	monoclinic	monoclinic	monoclinic
space group	*C*2/*c*	*C*2/*c*	$P2_1/n$
a [Å]	16.6780(49)	24.6364(41)	34.3934(8)
b [Å]	13.1034(37)	12.7192(42)	10.7163(17)
c [Å]	16.9087(39)	17.5405(39)	22.3647(7)
β [°]	121.16(2)	106.56(2)	106.895(3)
V [Å^3]	3162.2(16)	5268.4(23)	7895.1(8)
ρ_{calcd} [g cm^{-3}]	1.584	1.566	1.415
T [K]	293(2)	293(2)	293(2)
radiation, λ [Å]	$Mo_{K\alpha}$, 0.71073	$Mo_{K\alpha}$, 0.71073	$Mo_{K\alpha}$, 0.71073
monochromator	graphite	graphite	graphite
μ [mm^{-1}]	0.906	0.972	0.971
transmission min/max	0.702/0.850	–	–
scan type	$\omega - 2\theta$	$\omega - 2\theta$	$\omega - 2\theta$
θ range [°]	2–25	2–30	2–20
reflections measured	$-19 < h < 19$	$-34 < h < 34$	$-32 < h < 32$
	$-15 < k < 15$	$0 < k < 17$	$-11 < k < 11$
	$0 < l < 20$	$0 < l < 24$	$0 < l < 21$
standard reflections		3 every 400 reflections	
total reflns measured	5633	7907	6248
unique reflections	2782	7674	3735
R_{int}[a]	0.1037	0.0197	0.1300
refinement type	F^2	F^2	F^2
R_1[b]	0.0624 (1171 reflns)	0.0628(4224 reflns)	0.1110 (2028 reflns)
R_{all}	0.1569	0.1347	0.1970
wR_{2all}	0.1378	0.2077	0.2792
GOF[c]	0.877	1.010	1.087
refined parameters	214	361	471
weighting scheme[d]	$1/[\sigma^2F_o^2 + (0.0458P)^2 + 0.00P]$	$1/[\sigma^2F_o^2 + (0.104P)^2 + 6.7215P]$	$1/[^2F_o^2 + (0.0001P)^2 + 314.4P]$
$(shift/esd)_{max}$	0.000	0.001	0.000
max./min. $\Delta\rho$ [e Å^{-3}]	0.342/−0.477	0.826/−0.784	0.646/−0.386

[a] $R_{int} = \Sigma|F_o^2 - F_o^2(mean)|/\Sigma[F_o^2]$. [b] $R_1 = \Sigma||F_o| - |F_c||/\Sigma|F_o|$ (calculated on reflections with $I > 2\sigma_I$). [c] $GOF = S = [\Sigma[w(F_o^2 - F_c^2)^2]/(n-p)]^{0.5}$, where *n* is the number of reflections and *p* is the total number of parameters refined. [d] $P = [Max(F_o^2,0) + 2F_c^2)/3]$

featureless, thus confirming the reliability of the models. Nevertheless, these structural investigations must be considered as preliminary and they will be revised as soon as bigger crystals are available.

Calculations were performed with the WinGX software.[18] Correction for Lorentz polarization was applied for the three crystals. Empirical absorption correction was applied only for crystal $[Cu^{II}\mathbf{L}](CF_3SO_3)_2$; in the other two cases no suitable reflections for a ψ scan were found in the range $80^\circ < \phi < 90^\circ$. All the structures were solved by direct-methods (SIR92)[19] and refined by full-matrix least-squares using SHELXL.[20]

For crystal $[Cu^{I}_2\mathbf{L}_2](ClO_4)_2$ the non-hydrogen atoms were refined isotropically in order to reduce the number of parameters to be refined (only Cu and Cl atoms were refined anisotropically); the asymmetric unit of this crystal contains indeed 114 non-H atoms and for a better resolution of the structure a greater number of observed reflections would be necessary. In all the three structures the H atoms were inserted in the calculated positions with an isotropic atomic displacement parameter proportional to that of the neighbouring atom ($\times 1.2$) and not refined.

Atomic scattering factors were taken from *International Tables for X-ray Crystallography*.[21] Diagrams of the molecular structures were produced by the ORTEP program.[22]

Crystallographic data (excluding structure factors) for the structures reported in this paper have been deposited with the Cambridge Crystallographic Data Centre as supplementary publication no. CCDC 118957 ($[Cu^{II}\mathbf{L}](CF_3SO_3)_2$), CCDC 118958 ($[Cu^{I}_2\mathbf{L}_2](CF_3SO_3)_2$), CCDC 118959 ($[Cu^{I}_2\mathbf{L}_2](ClO_4)_2$). Copies of the data can be obtained free of charge on application to CCDC, 12 Union Road, Cambridge CB2 1EZ, UK (fax: (+44) 1223-336-033; e-mail: deposit@ccdc.cam.ac.uk).

Acknowledgment

This work has been financially supported by MURST (Progetto: Dispositivi Supramolecolari).

[1] a) M. Fujita, S. Nagao, K. Ogura, *J. Am. Chem. Soc.* **1995**, *117*, 1649; b) C. A. Hunter, *Angew. Chem.* **1995**, *107*, 1181; *Angew. Chem. Int. Ed. Engl.* **1995**, *34*, 1079; c) H. Rauter, I. Mutikainen, M. Blomberg, C. J. L. Lock, P. Amo-Ochoa, E. Freisinger, L. Randaccio, E. Zangrando, E. Chiarparin, B. Lippert, *Angew. Chem.* **1997**, *109*, 1353; *Angew. Chem. Int. Ed. Engl.* **1997**, *36*, 1296.

[2] P. Baxter, J.-M. Lehn, A. DeCian, J. Fischer, *Angew. Chem.* **1993**, *105*, 92; *Angew. Chem. Int. Ed. Engl.* **1993**, *32*, 69.

[3] a) P. N. W. Baxter, J.-M. Lehn, B. O. Kneisel, F. Fenske, *Angew. Chem.* **1997**, *109*, 2067; *Angew. Chem. Int. Ed. Engl.* **1997**, *36*, 1978; b) D. M. Bassani, J.-M. Lehn, K. Fromm, D. Fenske, *Angew. Chem.* **1998**, *110*, 2534; *Angew. Chem. Int. Ed.* **1998**, *37*, 2364.

[4] a) J.-M. Lehn, in *Supramolecular Chemistry*, VCH, Weinheim **1995**, p. 146; b) E. C. Constable, *Angew. Chem.* **1991**, *103*, 1482; *Angew. Chem. Int. Ed. Engl.* **1991**, *30*, 1450.

[5] a) A. P. de Silva, H. Q. N. Gunaratne, T. Gunnlaugsson, A. J. M. Huxley, C. P. McCoy, J. T. Rademacher, T. E. Rice, *Chem. Rev.* **1997**, *97*, 1515; b) L. Fabbrizzi, A. Poggi, *Chem. Soc. Rev.* **1995**, 197; c) G. W. Gokel, in *Crown Ethers and Cryptands*, RSC, Cambridge, **1991**, p. 151

[6] a) R. A. Bissel, E. Córdova, A. E. Kaifer, J. F. Stoddart, *Nature* **1994**, *369*, 133; b) A. Livoreil, C. O. Dietrich-Buchecker, J.-P. Sauvage, *J. Am. Chem. Soc.* **1994**, *116*, 9399; c) L. Fabbrizzi, F. Gatti, P. Pallavicini, E. Zambarbieri, *Chem. Eur. J.* **1999**, *5*, 682; d) G. De Santis, L. Fabbrizzi, D. Iacopino, P. Pallavicini, A. Perotti, A. Poggi, *Inorg. Chem.* **1997**, *36*, 827; e) P. R. Ashton, R. Ballardini, V. Balzani, S. E. Boyd, A. Credi, M. T. Gandolfi, M. Gómez-López, S. Iqbal, D. Philp, J. A. Preece, L. Prodi, H. G. Ricketts, J. F. Stoddart, M. S. Tolley, M. Venturi, A. J. P. White, D. J. Williams, *Chem. Eur. J.* **1997**, *3*, 152; f) V. Balzani, M. Gómez-López, J. F. Stoddart, *Acc. Chem. Res.* **1998**, *31*, 405–414; g) J.-P. Sauvage, *Acc. Chem. Res.* **1998**, *31*, 611–619.

[7] J.-P. Gisselbrecht, M. Gross, J.-M. Lehn, J.-P. Sauvage, R. Ziessel, C. Piccinni-Leopardi, J. M. Arrieta, G. Germain, M. V. Meersche, *Nouv. J. Chim.* **1984**, *8*, 661.

[8] a) K. T. Potts, M. Keshavarz-K, F. S. Tham, H. D. Abruña, C. R. Arana, *Inorg. Chem.* **1993**, *32*, 4422; b) K. T. Potts, M. Keshavarz-K, F. S. Tham, H. D. Abruña, C. R. Arana, *Inorg. Chem.* **1993**, *32*, 4436.

[9] J.-M. Lehn, J.-P. Sauvage, J. Simon, R. Ziessel, C. Piccinni-Leopardi, J.-P. Declercq, M. Van Meerssche, *Nouv. J. Chim.* **1983**, *7*, 413.

[10] K. T. Potts, K. A. Gheysen Raiford, M. Keshavarz-K, *J. Am. Chem. Soc.* **1993**, *115*, 2793.

[11] This angle is of course expected to be 60° in the free ligand (assuming *trans*-equatorial conformation). X-ray diffraction studies showed that, for the three different $[Cu^{I}_2\mathbf{L}_2]^{2+}$ molecular cations, the N–C–C–N torsion angle is 66.3° ($[Cu^{I}_2\mathbf{L}_2](ClO_4)_2$, helical form), 70.26° ($[Cu^{I}_2\mathbf{L}_2](ClO_4)_2$, nonhelical dimer) and 58.3° ($[Cu^{I}_2\mathbf{L}_2](CF_3SO_3)_2$).

[12] C. C. Phifer, D. R. McMillin, *Inorg. Chem.* **1986**, *25*, 1329.

[13] NMR spectra have been recorded also in CD_3OD. The results indicate that also in this solvent a mixture of a symmetric helix (prevalent: 100% at room temperature, 82% at $-30\,^\circ C$) and of an asymmetric one (0% at RT, 18% at $-30\,^\circ C$) exists.

[14] Attempts to isolate copper(II) complexes of $\mathbf{L}'$ as solids failed, owing to their much higher instability towards hydrolysis (Cu^{II} or Cu^{I}) and oxidation (Cu^{I}). However, the formation of the expected $[Cu^{I}\mathbf{L}'_2]^{+}$ and $[Cu^{II}\mathbf{L}'_2]^{2+}$ molecular cations has been checked by means of spectrophotometric titrations. In the case of both Cu^{I} and Cu^{II} typical bands (538 nm, $\varepsilon = 6350$, CT; 338 nm, $\varepsilon = 10250$, CT and 720, $\varepsilon = 88$, d–d, respectively) are observed, and the titration profiles display a clear stop at a metal/ligand molar ratio of 1:2.

[15] B. R. James, R. J. P. Williams, *J. Chem. Soc.* **1961**, 2007.

[16] T. Gennett, D. F. Milner, M. J. Weaver, *J. Phys. Chem.* **1985**, *89*, 2787.

[17] E. Cannillo, G. Germani, F. Mazzi, new crystallographic software for Philips PW 1100 single crystal diffractometer, *CNR Centro di Studio per la Cristallografia, Internal Report 2*, **1983**.

[18] L. J. Farrugia, WinGX-97, An Integrated System of Publicly Available Windows Programs for the Solution, Refinement and Analysis of Single-Crystal X-ray Diffraction, University of Glasgow, **1997**.

[19] A. Altomare, G. Cascarano, C. Giacovazzo, A. Gualardi, *J. Appl. Crystallogr.* **1993**, *26*, 343–350

[20] For crystals $[Cu^{II}\mathbf{L}](CF_3SO_3)_2$ and $[Cu^{I}_2\mathbf{L}_2](CF_3SO_3)_2$: GM Sheldrick, SHELXL-93, Program for Crystal Structure Refinement, University of Göttingen, Germany, **1993**; for crystal $[Cu^{I}_2\mathbf{L}_2](ClO_4)_2$: G. M. Sheldrick, SHELX-97, Programs for Crystal Structure Analysis, University of Gottingen, Germany, **1998**.

[21] *International Tables for X-ray Crystallography*, *Vol. 4* Kynoch, Birmingham, **1974**, pp. 99–101, 149–150.

[22] L. J. Farrugia, *J. Appl. Crystallogr.* **1997**, *30*, 565.

Received: April 26, 1999 [F1747]

